Molecular Catalysis 515 (2021) 111925

Contents lists available at ScienceDirect

Molecular Catalysis

journal homepage: www.journals.elsevier.com/molecular-catalysis

Conversion of levulinic acid to γ-valerolactone over Zr-containing metal-organic frameworks: Evidencing the role of Lewis and Brønsted acid sites

J.M. Guarinos [a], F.G. Cirujano [a,b], A. Rapeyko [a,*], F.X. Llabrés i Xamena [a,*]

[a] Instituto de Tecnología Química UPV-CSIC, Universitat Politècnica de València, Consejo Superior de Investigaciones Científicas, Avda. de los Naranjos, s/n, Valencia 46022, Spain
[b] Instituto de Ciencia Molecular (ICMOL), Universitat de Valencia, Catedrático José Beltrán Martínez n° 2, Valencia, Paterna 46980, Spain

ARTICLE INFO

Keywords:
Zirconium MOFs
MOF-808
UiO-66
Levulinic acid
Gamma-valerolactone

ABSTRACT

Zr-containing UiO-66 and MOF-808 are evaluated for converting levulinic acid (LA) into γ-valerolactone (GVL) through various routes: (i) Step-wise esterification of LA to *n*-butyl levulinate (*n*BuL) and Meerwein-Ponndorf-Verley (MPV) reduction to GVL; (ii) One-pot two-steps esterification with *n*-butanol followed by MPV reduction with *sec*-butanol; and (iii) direct conversion of LA into GVL through a tandem reaction. Selection of this multistep complex reaction evidences the participation of the different acid sites (Lewis or Brønsted) of the material in each individual step: Brønsted-induced acid sites catalyze esterification reaction efficiently, while Lewis acid sites are the preferred sites for the MPV step. Sulfation of MOF-808 is used to enhance the Brønsted acidity of MOF-808, which improves the performance for esterification. However, the sulfate groups introduced are detrimental for the MPV step, since they reduce the intra-pore space available to form the required bulky transition state. These results evidence the need to find the best equilibrium between Brønsted and Lewis acid sites to optimize the outcome of this multistep reaction.

Introduction

Levulinic acid (LA) is a largely available renewable compound that can be obtained from the deconstruction of lignocellulosic biomass [1]. LA is a versatile platform chemical for preparing many other important high value-added products in food and chemical industries, including alkyl levulinates and γ-valerolactone (4,5-Dihydro-5-methyl-2(3*H*)-furanone, hereafter GVL) [2]. GVL can be considered a sustainable hydrocarbon source for energy and chemicals [3]. The use of GVL as a renewable feedstock has attracted interest given the low toxicity and high stability of this compound. The low vapor pressure of GVL reduces the emission of volatile substances, which allows safe storage. On the other hand, GVL has a high chemical stability, preventing the hydrolysis to the acid form under neutral pH conditions and the formation of peroxides upon heating. These properties make GVL a very attractive compound as a fuel additive to produce cleaner-burning fuels, as a key intermediate in the synthesis of fine chemicals, such as adipic acid, valeric acid [4,5], or 5-nonanone [6], as a solvent, or as a component of biocide formulations [7]. Not surprisingly given the interest in GVL, several routes have been described for its preparation [8]. Most of them [9] are based on the conversion of LA or esther derivatives obtained from biomass using noble metal catalysts (Ru, Pt) and using H_2 or formic acid [10] as reducing agents. The process may take one of the following two routes: (i) reduction of LA to γ-hydroxyvaleric acid followed by intramolecular cyclization and dehydration; or (ii) acid-catalyzed dehydration of LA to angelica lactone (5-methyl-2(3*H*)-furanone) followed by hydrogenation of the C-C double bond (see Scheme 1). The first route is used when relatively low temperatures (typically less than 250 °C) are adopted in the absence of strong acid catalysts, while the second route occurs when higher temperatures (typically 300–350 °C) and strong mineral acids or solid acids are used.

The main drawback associated with the above methods for producing GVL from LA is the elevated cost of the noble metal catalysts used [11], along with the high pressures typically required (40–60 bar). On the other hand, the water content of the feed must be very low (less than *ca.* 2.5 wt%) to avoid metal leaching with the consequent loss of activity of the catalyst. To circumvent these limitations, other alternative routes to the synthesis of GVL from LA have been recently developed that are

* Corresponding authors.
E-mail addresses: arapeyko@itq.upv.es (A. Rapeyko), fllabres@itq.upv.es (F.X. Llabrés i Xamena).

https://doi.org/10.1016/j.mcat.2021.111925
Received 15 July 2021; Received in revised form 20 September 2021; Accepted 21 September 2021
Available online 3 October 2021

based on the chemoselective reduction of the keto group of LA by a Meerwein-Ponndorf-Verley (MPV) catalytic transfer hydrogenation reaction using a secondary alcohol as hydrogen source (see Scheme 2) [12,13]. Early reports described the use of both zirconium oxide [14] and Ni-Raney [15], thus avoiding the use of expensive noble metal catalysts. Meanwhile, the use of a secondary alcohol as a hydrogen source also avoids using H_2 as the reducing agent. However, both ZrO_2 and Ni Raney present also severe limitations, preventing their use for large scale GVL production. On one hand, the low MPV activity of ZrO_2 requires the use of an elevated amount of catalyst (up to twice the mass amount of LA) and a large alcohol excess (up to 155 mols of alcohol per mol of LA are needed to attain GVL yields higher than 90%). Also, the process only works smoothly when a levulinate ester is used as a starting product, while only a limited activity is observed when LA is directly used. This limitation introduces necessary previous esterification and separation steps of LA esters, complicating the preparation procedure of GVL. On the other hand, Ni Raney is used in an aqueous suspension, which difficult the management and the separation from GVL and presents health hazards. At the light of these results, it is evident that large scale conversion of LA into GVL through MPV reactions makes sense only if considerably more active catalysts are used.

A qualitative leap in this direction is represented by the introduction of tetravalent (Zr [16], Hf [17] or Sn [18]) or pentavalent (Nb or Ta [19]) metal cations in zeolites to produce highly active catalysts for MPV reduction of carbonyl compounds with secondary alcohols. In particular, Zr-and Hf-beta are good catalysts for preparing GVL from LA or its esters [17,20–22]. Metal-Organic Frameworks (MOFs) represent an interesting alternative to metal-containing zeolites as heterogeneous catalysts for MPV-type reactions. In particular, de Vos and co-workers [23] first demonstrated that Zr-containing UiO-66 [24] type MOFs can catalyze the conversion of geraniol with furfural, and this activity was improved by using a modulator synthesis approach [25]. Later, other Zr- and Hf-MOFs, such as MOF-808 [26–30] and DUT-67 [26], were also used as MPV catalysts [31,32]. In this sense, Valekar et al. [30], and Rojas-Buzo et al. [29] have reported the use of various Zr and Hf MOFs for the direct conversion of ethyl levulinate to GVL.

Herein, we comparatively evaluate the use of UiO-66 and MOF-808 (see the structure of these compounds in Fig. S1) as heterogeneous catalysts for the conversion of LA to GVL. We have considered various chemical routes: (i) A step-wise reaction (two-pots), consisting of esterification of LA to *n*-butyl levulinate (*n*BuL), followed by MPV reduction to GVL with *sec*-butanol; (ii) A one-pot two-steps process (without intermediate separation of products), using a linear alcohol (*n*-butanol) for the esterification and a secondary alcohol (*sec*-butanol) for the MPV; and (iii) A direct tandem esterification/MPV conversion of LA into GVL. Special emphasis is focused on disclosing the role of different types of acid sites (Lewis or Brønsted) in each reaction step, and to establish how these sites can be further modified in MOF-808 to improve the catalytic properties and optimize its performance.

Results and discussion

Brønsted-induced acidity in Zr-MOFs

We have recently shown that hydrated Zr-MOFs based on Zr_6 oxoclusters (such as UiO-66 and DUT-67) often possess Brønsted acidity related with strongly polarized H_2O molecules adsorbed onto (defective) Zr^{4+} sites [33]. Since both Brønsted acidity and hydration degree of the MOF are key factors determining their reactivity [34,35], it is necessary to determine whether these Brønsted-induced acid sites are present or not (and to what extent) in order to understand the catalytic properties of the compound. The Brønsted acid properties of a material can be directly determined by measuring the pH change of a solvent upon immersing the solid inside [36]. This can be carried out by potentiometric acid−base titrations, by dispersing the solid in an aqueous solution with a suitable electrolyte, such as $NaNO_3$ or NaCl, and allowing to equilibrate for several hours before the measurement [37]. However, potentiometric titrations in aqueous media cannot be used if we want to take into account the effects of the hydration degree of the solid. Alternatively, measurements in methanol can be carried out, following the procedure described before [33,38]. The results obtained for the Zr-MOFs studied in this work are summarized in Table 1.

As it can be seen in Table 1, when hydrated UiO-66 is dispersed in methanol, the pH decreases from 6.0 (for pure methanol) down to 2.2, thus evidencing the Brønsted acidity of the solid. This effect is less pronounced for the dehydrated material (pH = 4.0), which is in agreement with the origin of the Brønsted acidity to strongly coordinated water molecules, as discussed in detail elsewhere [33]. Conversely, dispersion of MOF-808 into methanol has almost no effect on the final pH of the solvent, regardless of whether it is hydrated or dehydrated. Therefore, it can be concluded that the Brønsted-induced acidity of MOF-808 is much less pronounced that in UiO-66. In order to increase the acidity of MOF-808, the solid was submitted to a sulfation process (see below). In this way, two new MOF-808 samples (labelled MOF-808-1.47SO_4 and MOF-808-2.63SO_4 in Table 1) were prepared with two different sulfation degrees. This sulfation process is well known to increase the Brønsted acidity of MOF-808, as first reported by Trickett et al. [35,39]. Accordingly, direct pH measurements in methanol revealed a noticeable decrease of the final pH of the dispersion depending on the sulfation degree of the solid, from 5.8 in as-prepared MOF-808, down to 3.0 and 2.0 for the sulfated solids (see Table 1). Note also that the acidity of sulfated MOF-808 is partially lost upon dehydration, similar to UiO-66 and in line with previous observations by Trickett et al. [35], evidencing the direct participation of water molecules in the Brønsted acid sites. Finally, it is important to stress that the Brønsted acidity of the MOFs is a surface effect; i.e., the pH is only lowered at the vicinity of the MOF particle. When the solid MOF was removed by filtration or centrifugation, the pH of the filtrate was virtually the same as that of pure methanol.

In order to complete the characterization of the acid properties of UiO-66 and MOF-808, and to confirm the observed effect of the hydration state of the sample, we have used solid-state ^{31}P magic-angle-spinning (MAS) NMR using trimethylphosphine oxide (TMPO) as probe molecule. A handful of examples exist on the use of phosphines and phosphine oxides as probe molecules adsorbed on MOFs [35,36,39,40], and they are widely employed for probing the acidic properties of other solid acid catalysts, such as zeolites [41], metal oxides [42,43], or heteropolyacids, and even ionic liquids and homogeneous catalysts [44,45]. In this study, we have selected TMPO because of its relatively small size (kinetic diameter ca. 0.55 nm) so it can readily enter the pores of both, UiO-66 and MOF-808 (pore openings of 0.6 and 1.4 nm, respectively, see Fig. S1) and interact with all the acid sites of the solid. TMPO interacts with both Brønsted and Lewis acid sites through the oxygen lone pairs, resulting in an upward ^{31}P chemical shift proportional to the acid strength of the center.

TMPO was first adsorbed from a CH_2Cl_2 solution on the UiO-66 sample with or without prior activation under a vacuum to remove adsorbed water, as detailed in the Experimental Section. The corresponding ^{31}P MAS NMR spectra obtained are compared in Fig. 1. In the spectrum of hydrated UiO-66, main peaks are observed at chemical

Table 1
pH values of stirred suspensions of various MOFs in methanol [a].

Catalyst	Hydrated	Dehydrated[b]
UiO-66	2.2	4.0
MOF-808	5.8	5.9
MOF-808-1.47SO_4	3.0	3.9
MOF-808-2.63SO_4	2.0	2.8
Blank (methanol alone)	6.0	

[a] pH of a stirred suspension of 6 mg of MOF in 24 mL of methanol, 25 °C. [b] The MOF was dried 12 h at 150 °C under vacuum before preparing the suspension in methanol.

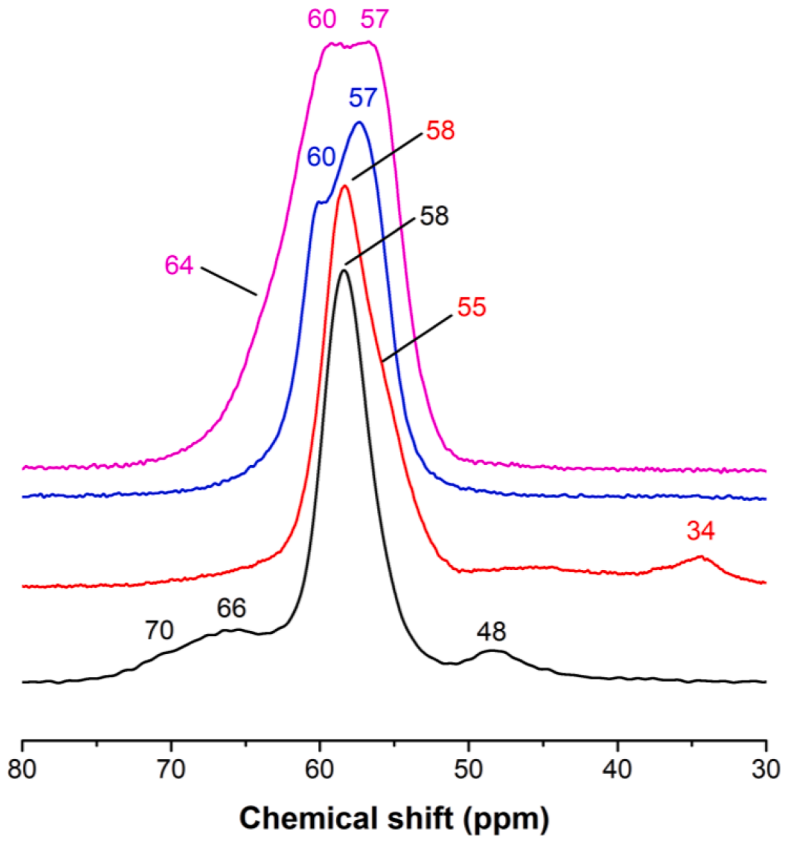

Fig. 1. ^{31}P MAS NMR spectra of TMPO adsorbed onto hydrated UiO-66 (*black curve*), dehydrated UiO-66 (*red curve*), hydrated MOF-808 (*blue curve*) and hydrated MOF-808-1.47SO_4 (*magenta curve*). (For interpretation of the references to colour in this figure legend, the reader is referred to the web version of this article.)

shifts of 70, 66, 58 and 48 ppm. While the latter peak can be readily attributed to free TMPO inside the pores, the peaks above 55 ppm correspond to TMPO adsorbed onto acid sites of increasing strength. Dehydration of UiO-66 brings about clear changes in the NMR spectrum, which is now dominated by a strong peak at 58 ppm (with a shoulder at 55 ppm) and a small peak at 34 ppm. Meanwhile, the peaks above 58 ppm that were present in hydrated UiO-66 are absent in the spectrum of the dehydrated sample. This clearly indicates that the strongest acid sites of UiO-66 are lost upon dehydration, in agreement with the direct pH measurements shown above, which evidence a definite diminution of the number of Brønsted acid sites in dehydrated UiO-66. Finally, the small peak at 34 ppm (which is below the chemical shift of 39 ppm expected for crystalline TMPO) has been previously attributed to "mobile" TMPO in the intracrystalline voids or weakly adsorbed near the pore openings [41].

Fig. 1 also shows the ^{31}P NMR spectrum obtained after adsorbing TMPO onto hydrated MOF-808. This spectrum contains two main peaks at 60 and 57 ppm, both associated to acid sites. Compared with hydrated UiO-66, these peaks appear at lower chemical shifts, which reveals the lower acid strength of the acid sites in MOF-808, in good agreement with the direct pH measurements in methanol. The spectrum of dehydrated MOF-808 (not shown) was identical to that of the hydrated compound. Finally, upon adsorption of TMPO onto MOF-808-1.47SO_4 the intensity of the peak at 60 ppm increases to equal the signal at 57 ppm, and a clear tail appears on the left hand side of the peak at ~ 64 ppm, revealing the higher acidity of the sulfated sample with respect to as-prepared MOF-808. The spectra obtained for both MOF-808 samples are analogous to those previously reported [39].

Despite both UiO-66 and MOF-808 having similar Zr_6 oxoclusters in their structures, the Brønsted-induced acid properties of the two compounds are completely different. This is because coordinatively unsaturated Zr^{4+} sites (*cus*) in both materials are also different. In UiO-66, Zr^{4+} vacancies are created when a terephthalate linker connecting two adjacent oxoclusters is lost (missing ligand defect). Consequently, two Zr^{4+} are coordinated to OH groups (to maintain the electrical neutrality of the material) and the other two are coordinated to one H_2O molecule each, as shown in Scheme 3. Conversely, in MOF-808 *cus* are created upon removal of the bridging formate ligands connecting two Zr ions in the same oxocluster. Since each Zr is initially connected to two formate ligands, the final material contains Zr^{4+} sites capped by one OH group and one H_2O molecule, simultaneously. Therefore, the effective polarizing power of the Zr^{4+} ions over the adsorbed water molecules is largely countered by the geminal OH groups. Hence, the Brønsted acidity of these coordinated H_2O molecules is much lower than in UiO-66, in which geminal OH groups are not present.

Once the acid properties of UiO-66 and MOF-808 have been characterized, we proceeded with the use of these compounds as acid catalysts for the conversion of LA into GVL. Different synthetic routes are explored, with the aim of determining the participation of each type of acid site (either Brønsted or Lewis) in the individual (trans)esterification and MPV steps.

Conversion of LA into GVL. First step: esterification of LA to nBuL

The first route explored for converting LA into GVL consisted in a two-steps process carried out in separate batch reactors. In the first step, LA is esterified with *n*-butanol (*n*-BuOH) to *n*BuL. Then, the *n*BuL formed in the first step, conveniently isolated and purified, is finally reduced to GVL through a MPV reaction using *sec*-butanol (*sec*-BuOH) as the secondary alcohol. This route has clear drawbacks, including the use of two different alcohols (one primary alcohol to accelerate the esterification step and one secondary alcohol to facilitate the MPV reaction); as well as the need of additional isolation and purification steps between the two steps. Obviously, this methodology involving multiple steps and

multiple solvents makes the process cost intensive and it is thus not feasible for the commercial production of a bulk chemical such as GVL. Nevertheless, it is still convenient from an academic point of view to evaluate this preparative route to gain valuable information on the participation of the different types of acid sites of the solid catalyst, both Lewis and Brønsted, as well as the existing differences between UiO-66 and MOF-808 catalysts. Note also that C4-alcohols were used for both esterification and MPV steps instead of a more convenient alternative such as isopropanol, due to their higher boiling points, which allowed us to carry out the reactions at higher temperatures to accelerate LA conversion.

We already reported the esterification of LA with *n*-BuOH using UiO-66 as catalyst [34,46]. Therefore, in the present work we have focused on MOF-808 to optimize the reactions conditions to maximize the yield of *n*BuL. The reaction parameters analyzed included the alcohol excess used, the catalyst loading, and the thermal pre-activation of the catalyst. All the reactions discussed in this work were carried out at 130 °C.

First, we analyzed the effect of the alcohol excess on the temporal distribution of products and final *n*BuL yields obtained. To do this, two LA:*n*-BuOH molar ratios of 1:6 and 1:22 were used. The results obtained are shown in Fig. S5 and Table 2.

In a preliminary blank experiment without any catalyst, a significant conversion of LA is obtained under the conditions used: 55% conversion after 24 h (entry 1 in Table 2), due to the autocatalytic role of LA and the relatively high reaction temperature used (130 °C). Nevertheless, in all cases the presence of the solid MOF catalysts afforded higher conversions, compared with the blank experiment. According to the time-conversion plots shown in Fig. S5, the reaction between LA and *n*-BuOH produces acetal in the first place, which reaches a maximum yield after 8 h of reaction and then it is progressively transformed into *n*BuL. However, this transformation is not complete even after 18 h of reaction, so that *n*BuL is not the sole product at the end of the reaction. By comparing the results obtained with the two LA:*n*-BuOH ratios, a large alcohol excess produces a slowdown of the reaction (TOF of 1.31 and 1.25 h^{-1}), increases the amount of acetal formed (up to ca. 18% yield after 8 h of reaction) and decreases the final yield of *n*BuL, from 82% to 60% for 1:6 and 1:22 ratios, respectively (compare entries 2 and 3).

Next, two different catalyst loadings were tested, corresponding to 9.3 and 18.7 mol% of zirconium with respect to LA. As shown in Table 2 (entries 3 and 4), the final *n*BuL yield increased from 82% (at 86% total LA conversion after 18 h of reaction) up to 94% *n*BuL yield (at 99% conversion after 14 h) for catalyst loadings of 9.3% and 18.7%, respectively.

For the sake of comparison, the esterification of LA with *n*-BuOH was also carried out over UiO-66 under the same conditions, using 18.7 mol % of Zr and a LA:*n*-BuOH molar ratio of 1:6. According with the results obtained, UiO-66 clearly outperformed MOF-808, with a much higher TOF (4.96 vs 1.50 h^{-1} for UiO-66 and MOF-808). Full conversion of LA wasattained after only 5 h, producing *n*BuL quantitatively as the sole reaction product (see entry 8).

As we discussed before, hydrated UiO-66 is more active in the esterification of LA with ethanol than the dehydrated material [33,34]. This is due to a relevant participation in the esterification reaction of the Brønsted-induced acid sites arising from strongly polarized water molecules adsorbed on Zr^{4+} *cus*. Upon dehydration of UiO-66, these polarized water molecules are removed and the Brønsted acidity of the material is largely lost, as revealed by direct pH measurements in methanol and ^{31}P NMR spectra of adsorbed TMPO (see above). We wanted to evaluate whether a similar effect of the pre-activation/dehydration was also observed for MOF-808. However, our results showed that the effect of the hydration state of MOF-808 is the opposite of what had been observed in UiO-66; i.e., the esterification of LA to *n*BuL is slightly slower (1.50 vs 0.82 h^{-1}) and less selective for hydrated than for dehydrated MOF-808 (compare entries 4 and 5 in Table 2).

The different behavior and opposite trend observed for hydrated and dehydrated UiO-66 and MOF-808 clearly points to a different participation of the active sites in both materials. While hydrated UiO-66 is a relatively strong Brønsted acid solid, the Brønsted acid sites in MOF-808 are considerably weak, so the esterification is more effectively catalyzed by its Lewis acid sites; i.e., Zr^{4+} *cus*. When MOF-808 is dehydrated during the pre-activation step, these Lewis acid sites become more exposed and available to catalyze the esterification reaction, and a slight increase of the catalytic activity is then observed.

We can thus conclude that in both materials esterification reactions are preferentially catalyzed by different types of acid: Strong Brønsted sites in the case of (hydrated) UiO-66 and Lewis sites in (dehydrated) MOF-808. Since UiO-66 is more active than MOF-808 (compare entries 4 and 8), then it can be concluded that Brønsted sites are more efficient than Lewis sites for the esterification reaction. We then reasoned that increasing the Brønsted acidity of MOF-808 could improve the catalytic activity of this material for the esterification reaction. One way to achieve this goal is by submitting MOF-808 to a sulfation process. According to Yaghi and co-workers, sulfation of MOF-808 can endow the material with superacid properties [35,39].

Indeed, as it is shown in Table 2, sulfation of MOF-808 produces a significant increase of the catalytic activity compared with the pristine material. This reinforces our assumption that Brønsted acid sites are the most effective catalytic sites for esterification. Moreover, the catalytic activity of two sulfated MOF-808 samples increases with the sulfation degree of the solid. Thus, MOF-808-1.47SO_4 produces full conversion of LA after 11 h of reaction (TOF = 2.23 h^{-1}), while MOF-808-2.63SO_4 requires only 5 h (TOF = 4.29 h^{-1}). Interestingly, the use of sulfated MOF-808 produced a small amount of GVL (up to 16%) as byproduct. Indeed, GVL was also formed in non-sulfated MOF-808, though to a much lower extend (< 2%). This result is a bit surprising since only a primary alcohol (*n*-BuOH) was present in the reaction medium. It is well known that MPV reactions are largely facilitated when a secondary alcohol is used as sacrificial hydride source.

Second step: MPV reduction of nBuL to GVL

Next, we studied the conversion of *n*BuL to GVL through a MPV reaction using *sec*-BuOH as the secondary alcohol. As in the first step, we

Table 2
Esterification of levulinic acid (LA) with *n*-butanol (*n*-BuOH) to produce *n*-butyl levulinate (*n*BuL) at $T = 130$ °C.

Entry	Catalyst	time (h)	LA:*n*-BuOH Molar ratio	Metal (mol%)	Conv.[a] (mol%)	TOF[b] (h^{-1})	Yield (mol%)[c]		
							acetal	*n*BuL	GVL
1	Blank	24	1:6	-	55	-	3	52	0
2	MOF-808	18	1:22	9.3	72	1.25	12	60	0
3	MOF-808	18	1:6	9.3	86	1.31	4	82	0
4	MOF-808	14	1:6	18.7	> 99	1.50	3	94	2
5	MOF-808[d]	14	1:6	18.7	78	0.82	3	73	2
6	MOF-808-1.47SO_4	11	1:6	18.7	> 99	2.23	1	83	16
7	MOF-808-2.63SO_4	11	1:6	18.7	97	4.29	0	91	6
8	UiO-66[c]	5	1:6	18.7	> 99	4.96	0	> 99	0

[a] Conversion of LA, determined by GC. [b] Turnover frequency: Moles of product converted per mol of catalyst and per hour, calculated at short reaction times. [c] Yields of the indicated products, determined by GC. [d] The catalyst was not pre-activated before the esterification reaction. GVL: γ-valerolactone.

also evaluated the effect of catalyst pre-activation, alcohol excess and catalyst loading. The results are summarized in Table 3.

Besides the expected formation of GVL, our catalytic results revealed that the reaction between *n*BuL and sec-BuOH produces also small amounts (<5 mol%) of *sec*-butyl levulinate (coming from a transesterification reaction) and the acetal of *sec*-butanol as byproducts.

As commented above, we have observed that catalyst pre-activation has an opposite effect on the reaction rate of esterification for UiO-66 and MOF-808: the reaction rate decreases in the first case, and increases in the latter. However, in the case of the MPV reaction, catalyst pre-activation improves the catalytic activity of the catalyst in all cases, both in MOF-808 and in UiO-66. This is because it is well-known that MPV requires Lewis acid sites, and dehydration of the catalyst by thermal activation improves the accessibility of these sites to the reaction substrates. Therefore, all the data shown in Table 3 correspond to pre-activated materials.

To determine the effect of the excess of *sec*-BuOH with respect to *n*BuL, two different molar ratios were used: 1:6 and 1:22. The larger alcohol excess (1:22 molar ratio) improves the catalytic results (compare entries 2 and 3), as opposite to what we observed for the esterification reaction. Likewise, increasing the catalyst loading from 9.3 to 18.7% is also beneficial for the reaction (entries 3 and 4).

As compared with MOF-808, UiO-66 presents a considerably lower catalytic activity (compare entries 4 and 7: TOFs of 2.10 vs. 0.03 h^{-1}). Thus, when MOF-808 was used as a catalyst, 95% conversion of *n*BuL was obtained after 12 h of reaction, with a 90% final yield of GVL. Conversely, with UiO-66 only 10% conversion of *n*BuL was obtained after 24 h and the reaction was less selective to GVL (40% of the *n*BuL converted was transformed into *sec*BuL through a transesterification reaction). In this sense, it is worth recalling than in UiO-66 the presence of coordinatively unsaturated Zr^{4+} sites depends on the amount of linker defects. Therefore, only a fraction of the total Zr ions present in the solid catalyst are accessible to substrate binding and can thus function as Lewis acid sites. Considering that the UiO-66 used in this work contained 9.5% of missing linkers, and that each missing linker molecule (terephthalate) creates two coordinatively unsaturated Zr^{4+}, it is inferred that a fraction of only 19% of the total zirconium ions can participate in the reaction. Conversely, all Zr^{4+} ions can participate in the reaction in MOF-808. If the TOF value reported for UiO-66 is recalculated taking into account only the accessible Zr^{4+} sites (19%), the value obtained (0.16 h^{-1}) is still much lower than that of MOF-808 (2.10 h^{-1}). Therefore, the availability of Zr^{4+} is not the only reason behind the lower activity of UiO-66 for the MPV reaction. It is worth recalling here that MOF-808 features considerable wider pores (adamantane-shaped cavities of 18.4 Å with apertures of 14 Å, see Fig. S1) than UiO-66 (octahedral cavities of *ca.* 11 Å and triangular windows of ca. 6 Å). Therefore, there is more space in the cavities of MOF-808 than in UiO-66 to accommodate the sterically demanding six-membered cyclic transition state of the MPV reaction (see Scheme 4). Both, the larger availability of Zr^{4+} ions and the presence of wider pores make MOF-808 a much more competent catalyst for the MPV reduction of *n*BuL than UiO-66. These results are in line with previous studies evidencing the superior behavior of MOF-808 with respect to UiO-66 in MPV reactions [26,27,29,30,33].

Finally, we have also analyzed the effect of sulfation of MOF-808 on the catalytic activity in the MPV reaction. As it is observed in Table 3, sulfation of MOF-808 is detrimental for this reaction, and the negative effect increases with the degree of sulfation. In this way, the deepest sulfated sample, MOF-808-2.63SO_4, produced 49% conversion of *n*BuL after 24 h (TOF = 0.38 h^{-1}), with 43% yield of GVL. These results somewhat improved for the less sulfated sample, MOF-808-1.47SO_4 (81% *n*BuL conversion and 76% GVL yield after 24 h, TOF = 1.05 h^{-1}), but they are still well below those obtained for the pristine MOF-808 (95% nBuL conversion and 90%GVL yield after 12 h, TOF = 2.10 h^{-1}). This is most likely related with the increased steric hindrance introduced by the sulfate groups inside the MOF cavities [35], which hampers the formation of the transition state of the MPV reaction. In any case, the increased Brønsted acidity of sulfated MOF-808 does not produce any significant increase of the formation of acetals, which remained in all cases below 5 mol%.

One-pot two-steps process

The next step in this study was to couple the two reactions, esterification and MPV, in a one-pot process, using two alcohols: a linear alcohol to facilitate the first esterification step, and a secondary alcohol as both solvent and hydride source to favor the MPV reaction in the second step. Coupling the two steps into a one-pot process avoids intermediate separation and isolation steps, which improves the process described above in two separate batch reactors. Nonetheless, the use of two different alcohols for the two steps is still a serious inconvenient for the practical viability of this catalytic route.

According to the previous results commented above, the one-pot two-steps process was carried out using 6 equivalents of *n*-BuOH with respect to LA in the first step, to minimize the formation of acetal, while 22 equivalents of *sec*-BuOH were used in the second step to accelerate the formation of GVL. The second alcohol was added directly to the reaction medium, without any separation or purification step, and once LA was quantitatively converted to *n*BuL. Note that this time varied from catalyst to catalyst, depending on the catalytic activity of each material for the esterification step. The addition of the second alcohol is indicated by a vertical line in Fig. 2. In all cases, the catalyst loading used was 18.7 mol% Zr and the reaction temperature was 130 °C. The results obtained are summarized in Table 4.

When hydrated UiO-66 was used as a catalyst, esterification reaction produced *n*BuL quantitatively as the sole product after 5 h (see Fig. 2a). However, when *sec*-BuOH was added to the reaction medium, the conversion of the *n*BuL formed in the first step was very slow. Only 8% yield of GVL was obtained after 21 h (26 h of total reaction time), mixed with about 4% of the transesterification product, *sec*-BuL (Table 4, entry 5). According to these results, UiO-66 does not seem to be a good catalyst for the one-pot two-steps synthesis of GVL from LA.

As discussed in the previous sections, MOF-808 is a better catalyst than UiO-66 for the MPV reaction, but it is worse for the esterification step. The overall performance of MOF-808 with respect to UiO-66 thus

Table 3
Meerwein-Ponndorf-Verley reduction of *n*-butyl levulinate (*n*BuL) with *sec*-butanol at $T = 130$ °C.

Entry	Catalyst	time (h)	*n*BuL:*sec*-BuOH Molar ratio	Metal (mol%)	Conv.[a] (mol%)	TOF[b] (h^{-1})	Yield (mol%)[c]		
							acetal	*sec*BuL	GVL
1	Blank	48	1:22	-	2	-	-	-	2
2	MOF-808	12	1:6	9.3	82	4.06	3	4	75
3	MOF-808	12	1:22	9.3	88	5.40	4	3	81
4	MOF-808	12	1:22	18.7	95	2.10	5	0	90
5	MOF-808-1.47SO_4	24	1:22	18.7	81	1.05	3	1	76
6	MOF-808-2.63SO_4	24	1:22	18.7	49	0.38	2	1	43
7	UiO-66	24	1:22	18.7	10	0.03	0	4	6

[a] Conversion of *n*BuL, determined by GC. [b] Turnover frequency: Moles of product converted per mol of catalyst and per hour, calculated at short reaction times [c] Yields of the indicated products, determined by GC. GVL: γ-valerolactone; *sec*BuL: *sec*-butyl levulinate.

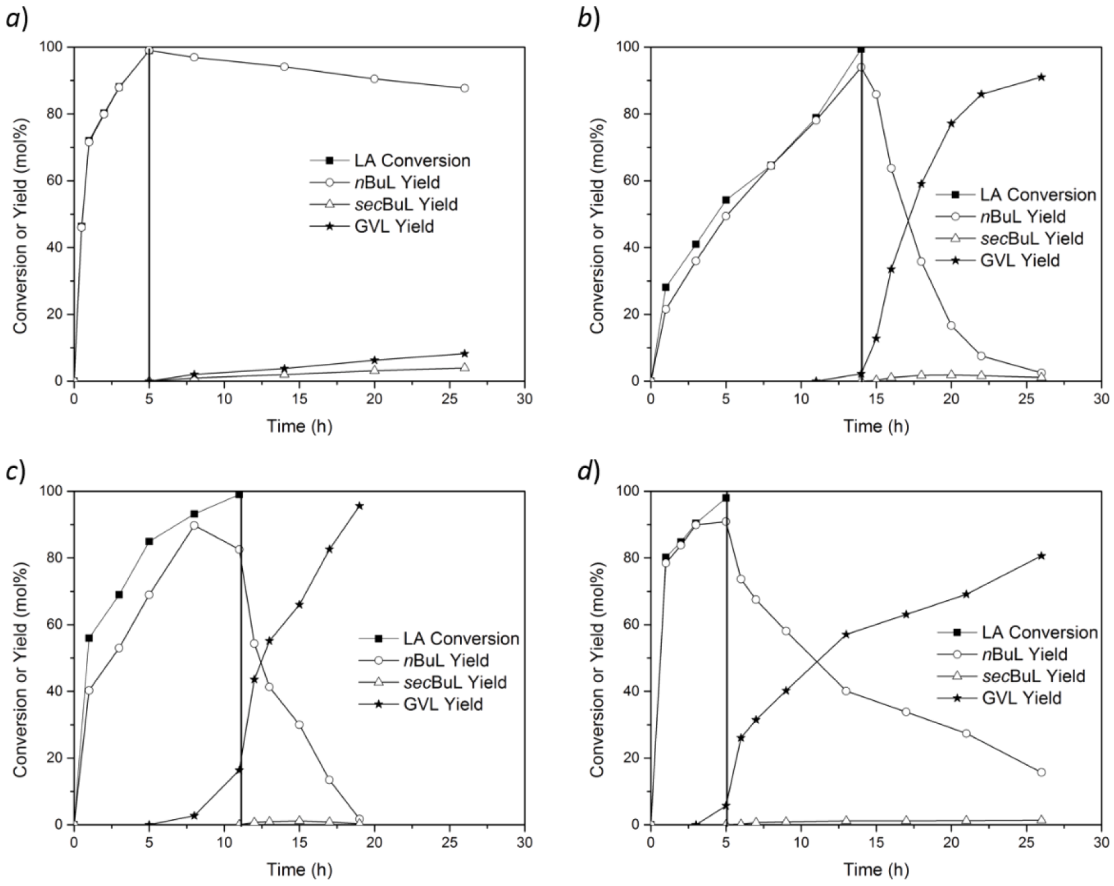

Fig. 2. One-pot two-steps conversion of LA over: (a) UiO-66; (b) MOF-808; (c) MOF-808-1.47SO_4; and (d) MOF-808-2.63SO_4. In all graphs, the vertical line indicates the end of the first step (esterification) and the addition of *sec*-BuOH to start the second step (MPV).

Table 4
One-pot two-steps conversion of LA to GVL [a].

Entry	Catalyst	time[b] (h)	Conv.[c] (mol%)	Yield (mol%)[d]			
				acetal	*n*BuL	*sec*BuL	GVL
1	Blank	-	-	-	-	-	-
2	MOF-808	26	> 99	5	3	1	91
3	MOF-808-1.47SO_4	19	> 99	2	2	0	96
4	MOF-808-2.63SO_4	26	> 99	1	16	2	81
5	UiO-66	26	> 99	0	88	4	8

[a] Reaction conditions: LA: *n*-BuOH molar ratio = 1:6 (*first step*); LA: *sec*-BuOH molar ratio = 1:22 (*second step*); catalyst loading 18.7 mol% Zr, T = 130 °C.
[b] Total reaction time (*first step* + *second step*).
[c] Conversion of LA, determined by GC.
[d] Yields of the indicated products, determined by GC. *n*BuL: *n*-butyl levulinate; *sec*BuL: *sec*-butyl levulinate; GVL: γ-valerolactone.

depends on the balance between these two opposite effects. As it is observed in Fig. 2b and Table 4, the esterification reaction over MOF-808 took up to 14 h to complete, but the ensuing MPV step was very effective. The overall one-pot two-steps process was accomplished after 26 h of total reaction time and GVL was obtained with a final yield of 91%, mixed with small traces of transesterification product (1% yield *sec*BuL) and unreacted *n*BuL from the first step (3%). Therefore, MOF-808 was overall a better catalyst than UiO-66 for this process.

With respect to pristine MOF-808, the sample with the lowest sulfation degree, MOF-808-1.47SO_4, produced better results for the one-pot two steps process: 96% GVL yield was obtained after only 19 h of reaction (Fig. 2c). However, the catalytic results were worse when the deepest sulfated sample was used, MOF-808-2.63SO_4. As it can be seen in Fig. 2d, the esterification reaction was very fast (< 5 h), but the MPV was significantly slower. Overall, the acceleration in the first step does not compensate the slowdown of the MPV. A maximum GVL yield of 81% is obtained after 26 h, as compared to the 96% obtained with MOF-808-1.47SO_4 after 19 h. These results evidence the need to find the best equilibrium between Brønsted and Lewis acid sites to optimize the outcome of this multistep reaction.

Direct conversion of levulinic acid to γ-valerolactone

Finally, we studied the direct conversion of LA to GVL through a MPV reaction using *sec*-BuOH as the secondary alcohol. One of the main limitations of existing reports so far on GVL synthesis through a MPV reaction is the relatively low activity of most catalysts when LA is used as the starting product. Most of them require the use of levulinate esters as more suitable precursors. Obviously, the direct conversion of LA to MPV in one-pot represents a clear improvement towards process intensification. Moreover, the direct conversion of LA to GVL requires using only one alcohol for the whole process, thus improving the atom economy of the process.

Based upon the previous reactions studied above, the following reaction conditions were selected: 18.7 mol% of pre-activated catalysts with respect to LA, a 1:22 LA:*sec*-BuOH molar ratio and a reaction temperature of 130 °C. A summary of the results is presented in Table 5, while Fig. 3 shows the corresponding kinetic data.

As it can be seen in Fig. 3b, full LA conversion was obtained after 70 h of reaction over MOF-808, with an overall 97% yield of GVL. At short reaction times, a small fraction (below 10 mol%) of the ester product, *sec*BuL was formed but it was progressively converted to GVL.

Table 5
Direct conversion of levulinic acid into γ-valerolactone [a].

Entry	Catalyst	Conversion[b] (mol%)	Yield (mol%)[c]		
			acetal	*sec*BuL	GVL
1	Blank	20	17	3	0
2	MOF-808	100	3	0	97
3	MOF-808-1.47SO_4	100	5	12	83
4	MOF-808-2.63SO_4	84	1	70	13
5	UiO-66	67	1	56	10

[a] 18.7 mol% of pre-activated catalysts with respect to LA, a 1:22 LA:*sec*-BuOH molar ratio and reaction temperature of 130 °C were used in all cases. The conversion and yield data correspond to 70 h of reaction time. [b] Conversion of LA, determined by GC. [b] Yields of the indicated products, determined by GC. GVL: γ-valerolactone; *sec*BuL: *sec*-butyl levulinate.

Conversely, when UiO-66 was used the LA conversion was only 67% after the same reaction time, and the product evolution was completely different, being the ester the main product and the final GVL yield as low as 10% (Fig. 3a and entry 5 in Table 5). Therefore, MOF-808 is far more competent than UiO-66 for the direct production of GVL from LA.

As far as the sulfated MOF-808 are concerned, their catalytic activity for the production of GVL was bad compared with the pristine MOF-808. Moreover, the results were worse when the degree of sulfation increased: the increased Brønsted acidity of the solid introduced upon the sulfation process clearly favors the formation of the intermediate *sec*BuL over GVL, as expected. Note that in the case of MOF-808-1.47SO_4 (relatively low Brønsted acidity) the time evolution of products resembles that of MOF-808, while in MOF-808-1.47SO_4 (stronger Brønsted acidity) it is more similar to UiO-66.

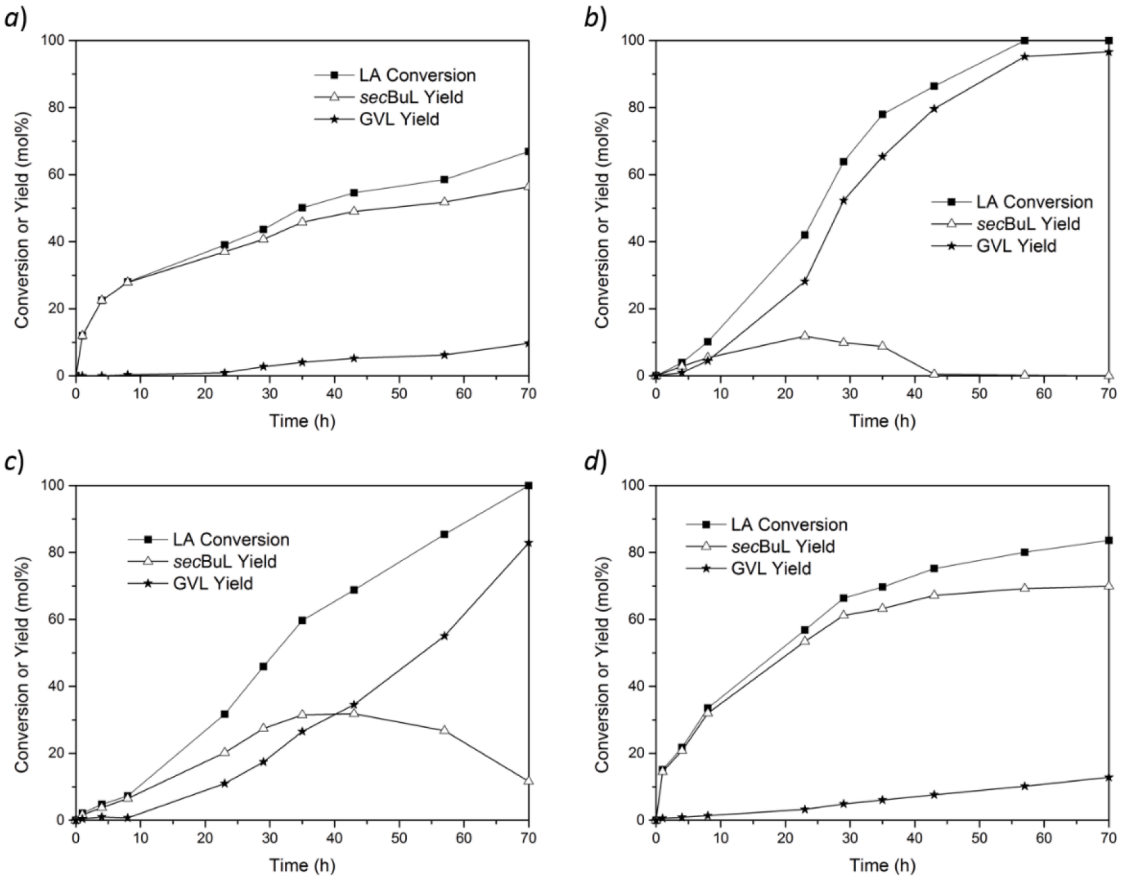

Fig. 3. Direct reaction of LA with sec-BuOH over: (a) UiO-66; (b) MOF-808; (c) MOF-808-1.47SO_4; and (d) MOF-808-2.63SO_4.

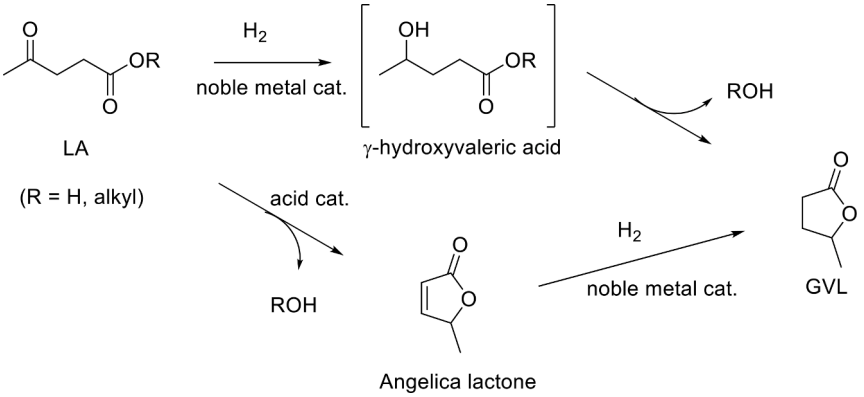

Scheme 1. Synthesis of GVL from LA using acid/hydrogenation catalysts.

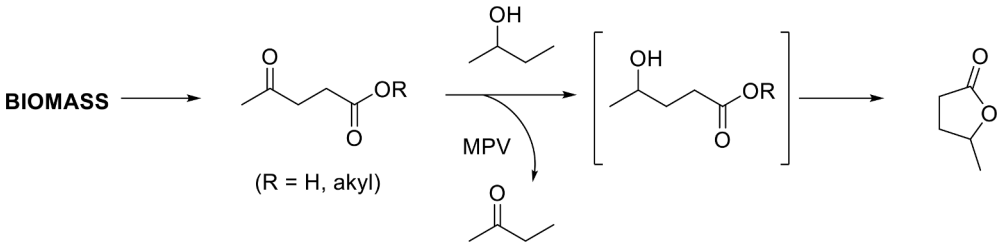

Scheme 2. Alternative synthesis of GVL through a tandem esterification/Meerwein-Ponndorf-Verley (MPV) reaction.

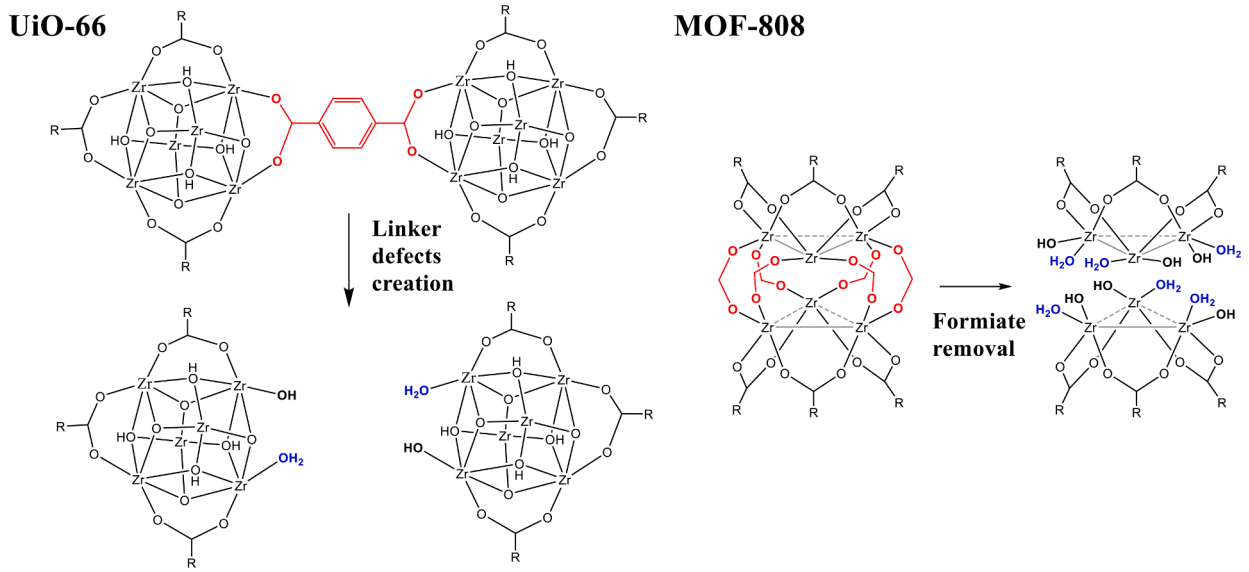

Scheme 3. Creation of Brønsted-induced sites (H_2O molecules coordinated to Zr^{4+} sites, depicted in blue) in UiO-66 and MOF-808. (For interpretation of the references to colour in this figure legend, the reader is referred to the web version of this article.)

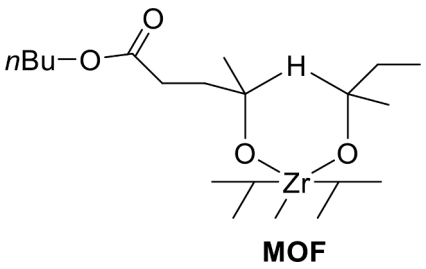

Scheme 4. Proposed six-membered cyclic transition state for the MPV reduction of nBuL with sec-BuOH over Zr-MOFs, involving the participation of Zr^{4+} Lewis acid sites.

Stability and reusability of MOF-808

Finally, we wanted to check the stability and reusability of MOF-808 for the direct conversion of LA to GVL. To do so, the reaction was carried out for three consecutive cycles, and the LA conversion and GVL/*sec*-BuL yields obtained after 23 h were compared. After this reaction time, LA conversions of around 40% were obtained, which allowed us a fair appraisal of eventual catalyst deactivation. In all cases, full LA conversion was attained after 70 h of reaction. Between two consecutive catalytic cycles, the solid catalyst was washed with *sec*-BuOH, dried at room temperature and pre-activated at 150 °C under vacuum overnight before the next cycle.

As shown in Fig. S6, a small decrease of both LA conversion and GVL yield was observed between the first and the second reuse, but the activity is stable for the ensuing cycle. This initial decrease of activity is most likely due to both, a progressive deterioration of the crystalline structure of the MOF and to the irreversible adsorption of reaction products on the surface of the solid. This adsorbates are not completely removed during the washing and pre-activation process, and partially block the active sites of the catalyst. Note that the effect of the pore clogging upon reuse has a little or no effect on the production of the ester, *sec*BuL, while it severely decreases the formation of GVL, whose transition state is more spatially demanding. Meanwhile, the crystallinity of MOF-808 is preserved during the catalytic use, acccording to the X-ray diffractogram of the solid recovered after the last catalytic cycle (see Fig. S7 in the Supporting Information), while the specific surface area of the material recovered after three catalytic runs is lowered by *ca.* 20% with respect to pristine MOF-808 (from 1542 to 1215 m^2g^{-1}. see Fig. S8), in line with the partial pore clogging commented above. The presence of adsorbed products on the solid after the catalytic reaction is clearly evidenced by comparing TGA and FTIR spectra with those of the fresh catalyst (see Figs. S9 and S10).

Conclusions

Herein we have studied in detail the conversion of LA into GVL over two Zr-containing MOFs: UiO-66 and MOF-808. Three different routes have been considered: (i) Step-wise conversion of LA into *n*BuL followed by MPV reduction to GVL in two separate reactors; (ii) One-pot two-steps reaction (without intermediate purification of intermediates) using a linear alcohol (*n*-BuOH) for the esterification and a secondary alcohol (*sec*-BuOH) for the MPV; and (iii) Direct tandem esterification/MPV conversion of LA into GVL using *sec*-BuOH.

Despite their chemical similarities regarding the presence of Zr_6

hexanuclear inorganic nodes, the two MOFs behave differently, based upon the type of acidity (Lewis or Brønsted) of the material. While (hydrated) UiO-66 possesses strong Brønsted acidity arising from strongly polarized H_2O adsorbed on Zr^{4+} defective sites, the acidity of MOF-808 comes mainly from their Zr^{4+} *cus*, acting as Lewis acid sites. Since LA esterification is favored by strong Brønsted acid sites, UiO-66 is more active than MOF-808 in this reaction. However, MPV reaction is more efficiently catalyzed by Lewis acid sites, and therefore the opposite trend in reactivity is observed.

Given the preferred participation of Brønsted acid sites in the esterification reaction, we have submitted MOF-808 to a sulfation process, as a means to improve its Brønsted acidity as well as the catalytic activity in this reaction. However, sulfation of MOF-808 has a negative effect on the catalytic activity for the MPV reaction, since it decreases the pore space available to form the required bulky six-membered transition state. These results evidence the need to find the best equilibrium between Brønsted and Lewis acid sites to optimize the outcome of a multistep reaction such as the formation of GVL from LA. This can be achieved by the judicious selection of the most appropriate material (UiO-66 or MOF-808), catalyst pre-treatment (activation/dehydration) or post-synthesis treatment (e.g., sulfation)..

Experimental section

Synthesis of Zr MOFs

UiO-66 was prepared using the method reported by Kandiah et al. with slight modifications [47]. Briefly, $ZrCl_4$ (375 mg, 1.6 mmol) was dissolved in 25 mL of *N,N*-dimethylformamide (DMF) and 1,4-benzenedicarboxylic acid (BDC) was dissolved in 20 mL of DMF. Then, both solutions were sonicated during 15 min at ambient temperature and mixed inside a screw-capped glass bottle. The resulting mixture was placed in the oven at 80 °C during 24 h and then the temperature was raised to 100 °C and the mixture was kept for another 24 h. The resulting white precipitate was recovered by filtration under vacuum and washed with DMF and CH_2Cl_2. Finally, the obtained solid was dried under vacuum at ambient temperature. The as-prepared sample contained 9.5% of missing linker defects, as determined by the procedure indicated in the Supporting Information.

MOF-808 was prepared following the procedure described by Furukawa et al. [48] with slight modifications. First, 728 mg of $ZrOCl_2 \bullet 8H_2O$ was dissolved in 44.8 mL of formic acid-DMF solvent mixture with 3:1 (v/v) ratio. Then, 316 mg of trimesic acid (BTC) was dissolved in 22.4 mL of DMF. Both solutions were mixed and placed in a Teflon lined autoclave. Then, the autoclave was introduced into an oven at 130 °C for 48 h. After cooling down to room temperature the material was recovered by centrifugation. Finally, the obtained solid was washed 3 times with DMF (changing the solvent every 15 min) and 3 times with ethanol (changing the solvent every 30 min). After removing the solvent by centrifugation the solid was dried in air at ambient temperature.

MOF-808-1.47SO$_4$ was prepared following the method described by Jiang et al.[39] MOF-808 prepared by the method described above was first activated at 150 °C under vacuum during 16 h. Then, 134 mg of activated MOF-808 was suspended in 14 mL of 0.005 M H_2SO_4 for 24 h, during which time the mixture was stirred once every 2 h. The material thus obtained was solvent exchanged with miliQ water for 6 h (changing the solvent every 2 h), then quickly exchanged with acetone (5 times) and finally suspended in chloroform for 6 h (changing the solvent every 2 h). After that, the chloroform was removed by filtration and the resulting material was dried under vacuum at ambient temperature. The number "1.47" in the sample name indicates the degree of sulfation of the sample, as calculated by the procedure indicated in the Supporting Information.

MOF-808-2.63SO$_4$ was prepared using the same procedure as for MOF-808-1.47SO_4 but using 0.01 M H_2SO_4 aqueous solution to get a higher grade of sulfation of MOF.

Characterization of MOFs

All synthetized MOFs were characterized by Powder X-ray diffraction (Phillips X'Pert, Cu Kα radiation) to confirm the expected structure and high crystallinity of the materials. XRD diffraction patterns of all synthetized MOFs are shown in Fig. S2 (see SI).

Textural properties were determined by N_2 adsorption-desorption experiments at 77 K after outgassing the solids at 423 K overnight using a Micromeritics ASAP 2420 instrument. The isotherms obtained and calculated specific surface areas (S_{BET}) are shown in Fig. S3.

Thermogravimetric analysis (TGA) of the synthetized MOFs was performed under a flow of air and a heating ramp of 10°C min^{-1} using a NETZSCH STA 449 F3 Jupiter analyzer. TG and derivative curves (DTG) are presented in Fig. S4. Elemental microanalysis (CNHS) of the as-synthetized MOFs was performed in a EuroEA3000 CHNS-O Analyzer. The results of elemental analysis are presented in the Table S1.

The metal content of the MOFs was determined by both Inductively Coupled Plasma-Optical Emission Spectroscopy (ICP-OES) analysis using Varian 715-ES equipment, and from the corresponding TGA curves, in which the solid residue corresponded to ZrO_2, as confirmed by XRD. The results of Zr content obtained by both techniques coincide fairly well, as shown in Table S1 (see SI).

Adsorption of trimethylphosphine oxide (TMPO) was carried out as follows. The solid catalyst (30 mg), either as-prepared or pre-activated at 150 °C under a vacuum for 18 h to remove adsorbed water, was contacted with a CH_2Cl_2 solution (1 mL) of TMPO (0.074 mg TMPO/mg of solid) at room temperature. The mixture was allowed to equilibrate at room temperature for 4 h and the excess of CH_2Cl_2 was eliminated under a vacuum at room temperature. ^{31}P MAS NMR spectra were recorded on a Bruker Avance III HD 400 spectrometer using a 3.2 mm probe, with a spinning rate of 15 kHz and a recycle delay of 20 s. A $\pi/2$ pulse length of 4.5 μs was used with proton decoupling (spinal 64) during acquisition. Chemical shifts are reported in ppm relative to H_3PO_4.

Catalytic experiments

Esterification of levulinic acid with n-butanol. Esterification reactions were performed in batch reactors using the following procedure: 0.9 mmol of levulinic acid, the required amount of *n*-butanol and the solid MOF were placed in a closed glass tube reactor. The reaction was carried out under stirring at 130 °C and followed by taking sample aliquots at regular time periods. The reaction samples were analyzed by GC (Varian 3900) with a P20(WAX) column (15 m long, i.d. 0.32 mm) using dodecane as internal standard. All products were identified by mass spectrometry analysis. The amounts of alcohol and MOF were varied and specific conditions for each reaction are presented in the footnotes of the corresponding graphics and tables. When indicated, activation of the MOFs was carried out at 150 °C under vacuum during 18 h before reaction.

Synthesis of GVL from n-butyl levulinate through a MPV reduction. The MPV reaction was carried out using the following procedure: 0.9 mmol of *n*-butyl levulinate, the required amount of *sec*-butanol and the solid MOF were placed in a glass tube reactor. The reaction mixture was carried out under stirring at 130 °C taking sample aliquots at regular time periods. The reaction was followed by GC (Varian 3900) with a P20 (WAX) column (15 m long, i.d. 0.32 mm) and using dodecane as internal standard. All products were identified by mass spectrometry analysis. The amounts of alcohol and MOF were varied and specific conditions for each reaction are presented in the footnotes of corresponding graphics and tables. When indicated, activation of the MOFs was carried out at 150 °C under vacuum during 18 h before reaction.

One-pot two-steps conversion of levulinic acid into GVL. Levulinic acid was converted into GVL by a one-pot two-steps esterification-MPV process. In the first step, esterification of LA with *n*-butanol was carried out using the following procedure: 0.9 mmol of levulinic acid, 6 mmol of *n*-butanol and MOF (18.7 mol.%) were placed in a glass tube

reactor. The reaction was carried out under magnetic stirring at 130 °C. Once LA was totally converted, *sec*-butanol (22 mmol) was added to the reaction to trigger the MPV reaction (second step). Reaction samples were taken at regular time periods and analyzed by GC (Varian 3900) with a P20 (WAX) column (15 m long, i.d. 0.32 mm) using dodecane as internal standard. All products were identified by mass spectrometry analysis. When indicated, activation of the MOFs was carried out at 150 °C under vacuum during 18 h before reaction.

Direct synthesis of GVL from LA and sec-butanol. The one-pot reaction was performed using the following procedure: 0.9 mmol of LA, 22 mmol of *sec*-butanol and MOF (18.7 mol.%) were placed in a glass tube reactor. The reaction mixture was magnetically stirred at 130 °C in a closed reactor. The reaction samples were analyzed by GC (Varian 3900) with a P20(WAX) column (15 m long, i.d. 0.32 mm) using dodecane as internal standard. All products were identified by mass spectrometry analysis.

CRediT authorship contribution statement

J.M. Guarinos: Investigation, Validation, Formal analysis, Writing – original draft. **F.G. Cirujano:** Investigation, Methodology. **A. Rapeyko:** Methodology, Writing – review & editing, Supervision. **F.X. Llabrés i Xamena:** Conceptualization, Methodology, Writing – review & editing, Supervision.

Declaration of Competing Interest

The authors declare that they have no known competing financial interests or personal relationships that could have appeared to influence the work reported in this paper.

Acknowledgments

Financial support by the Spanish Government is acknowledged through projects MAT2017-82288-C2-1-P and the Severo Ochoa program (SEV-2016-0683). Aula-CEMEX is also acknowledged for a fellowship to JMG.

Supplementary materials

Supplementary material associated with this article can be found, in the online version, at doi:10.1016/j.mcat.2021.111925.

References

[1] A. Corma Canos, S. Iborra, A. Velty, Chemical routes for the transformation of biomass into chemicals, Chem. Rev. 107 (2007) 2411–2502, https://doi.org/10.1021/cr050989d.
[2] J. Zhang, S. Wu, B. Li, H. Zhang, Advances in the catalytic production of valuable levulinic acid derivatives, ChemCatChem. 4 (2012) 1230–1237, https://doi.org/10.1002/cctc.201200113.
[3] I.T. Horváth, H. Mehdi, V. Fábos, L. Boda, L.T. Mika, γ-Valerolactone—a sustainable liquid for energy and carbon-based chemicals, Green Chem. 10 (2008) 238–242, https://doi.org/10.1039/b712863k.
[4] R. Palkovits, Pentenoic acid pathways for cellulosic biofuels, Angew. Chem. Int. Ed. 49 (2010) 4336–4338, https://doi.org/10.1002/anie.201002061.
[5] J.P. Lange, R. Price, P.M. Ayoub, J. Louis, L. Petrus, L. Clarke, H. Gosselink, Valeric biofuels: a platform of cellulosic transportation fuels, Angew. Chem. Int. Ed. 49 (2010) 4479–4483, https://doi.org/10.1002/anie.201000655.
[6] J.C. Serrano-Ruiz, D. Wang, J.A. Dumesic, Catalytic upgrading of levulinic acid to 5-nonanone, Green Chem. 12 (2010) 574–577, https://doi.org/10.1039/b923907c.
[7] D. Fegyverneki, L. Orha, G. Láng, I.T. Horváth, Gamma-valerolactone-based solvents, Tetrahedron 66 (2010) 1078–1081, https://doi.org/10.1016/j.tet.2009.11.013.
[8] J.C. Serrano-Ruiz, R.M. West, J.A. Dumesic, Catalytic conversion of renewable biomass resources to fuels and chemicals, Annu. Rev. Chem. Biomol. Eng. 1 (2010) 79–100, https://doi.org/10.1146/annurev-chembioeng-073009-100935.
[9] W.R.H. Wright, R. Palkovits, Development of heterogeneous catalysts for the conversion of levulinic acid to γ-valerolactone, ChemSusChem. 5 (2012) 1657–1667, https://doi.org/10.1002/cssc.201200111.
[10] X.L. Du, L. He, S. Zhao, Y.M. Liu, Y. Cao, H.Y. He, K.N. Fan, Hydrogen-independent reductive transformation of carbohydrate biomass into γ-valerolactone and pyrrolidone derivatives with supported gold catalysts, Angew. Chem. Int. Ed. 50 (2011) 7815–7819, https://doi.org/10.1002/anie.201100102.
[11] T.E. Graedel, On the future availability of the energy metals, Annu. Rev. Mater. Res. 41 (2011) 323–335, https://doi.org/10.1146/annurev-matsci-062910-095759.
[12] M.M. Antunes, A.F. Silva, A. Fernandes, A.A. Valente, γ-Valerolactone synthesis from α-angelica lactone and levulinic acid over biobased multifunctional nanohybrid catalysts, Catal. Today. (2021), https://doi.org/10.1016/j.cattod.2021.08.027. In press.
[13] C. Xu, E. Paone, D. Rodrí Guez-Padró, R. Luque, F. Mauriello, Recent catalytic routes for the preparation and the upgrading of biomass derived furfural and 5-hydroxymethylfurfural, Chem. Soc. Rev. 49 (2020) 4273, https://doi.org/10.1039/d0cs00041h.
[14] M. Chia, J.A. Dumesic, Liquid-phase catalytic transfer hydrogenation and cyclization of levulinic acid and its esters to γ-valerolactone over metal oxide catalysts, Chem. Commun. 47 (2011) 12233–12235, https://doi.org/10.1039/c1cc14748j.
[15] Z. Yang, Y.B. Huang, Q.X. Guo, Y. Fu, Raney® Ni catalyzed transfer hydrogenation of levulinate esters to γ-valerolactone at room temperature, Chem. Commun. 49 (2013) 5328–5330, https://doi.org/10.1039/c3cc40980e.
[16] Y. Zhu, G. Chuah, S. Jaenicke, Chemo- and regioselective Meerwein–Ponndorf–Verley and Oppenauer reactions catalyzed by Al-free Zr-zeolite beta, J. Catal. 227 (2004) 1–10, https://doi.org/10.1016/j.jcat.2004.05.037.
[17] H.Y. Luo, D.F. Consoli, W.R. Gunther, Y. Román-Leshkov, Investigation of the reaction kinetics of isolated Lewis acid sites in Beta zeolites for the Meerwein–Ponndorf–Verley reduction of methyl levulinate to g-valerolactone, J. Catal. 32 (2014) 198–207, https://doi.org/10.1016/j.jcat.2014.10.010.
[18] A. Corma, M.E. Domine, L. Nemeth, S. Valencia, Al-Free Sn-Beta Zeolite as a Catalyst for the Selective Reduction of Carbonyl Compounds (Meerwein-Ponndorf-Verley Reaction), J. Am. Chem. Soc. 124 (2002) 3194–3195, https://doi.org/10.1021/ja012297m.
[19] A. Corma, F.X. Llabrés i Xamena, C. Prestipino, M. Renz, S. Valencia, Water Resistant, Catalytically Active Nb and Ta Isolated Lewis Acid Sites, Homogeneously Distributed by Direct Synthesis in a Beta Zeolite, J. Phys. Chem. C 113 (2009) 11306–11315, https://doi.org/10.1021/jp902375n.
[20] M. Chia, J.A. Dumesic, Liquid-phase catalytic transfer hydrogenation and cyclization of levulinic acid and its esters to c-valerolactone over metal oxide catalysts, Chem. Commun. 47 (2011) 12233–12235, https://doi.org/10.1039/c1cc14748j.
[21] L. Bui, H. Luo, W.R. Gunther, Y. Román-Leshkov, Domino Reaction Catalyzed by Zeolites with Brønsted and Lewis Acid Sites for the Production of g-Valerolactone from Furfural, Angew. Chem. Int. Ed. 52 (2013) 8180–8183, https://doi.org/10.1002/anie.201302575.
[22] J. Wang, S. Jaenicke, G.K. Chuah, Zirconium–Beta zeolite as a robust catalyst for the transformation of levulinic acid to g-valerolactone via Meerwein–Ponndorf–Verley reduction, RSC Adv. 4 (2014) 13481–13489, https://doi.org/10.1039/c4ra01120a.
[23] F. Vermoortele, M. Vandichel, B. Van de Voorde, R. Ameloot, M. Waroquier, V. Van Speybroeck, D.E. de Vos, Electronic Effects of Linker Substitution on Lewis Acid Catalysis with Metal–Organic Frameworks, Angew. Chem. Int. Ed. 51 (2012) 4887–4890, https://doi.org/10.1002/anie.201108565.
[24] J.H. Cavka, S. Jakobsen, U. Olsbye, N. Guillou, C. Lamberti, S. Bordiga, K. P. Lillerud, A New Zirconium Inorganic Building Brick Forming Metal Organic Frameworks with Exceptional Stability, J. Am. Chem. Soc. 130 (2008) 13850–13851, https://doi.org/10.1021/ja8057953.
[25] F. Vermoortele, B. Bueken, G.Le Bars, B. Van de Voorde, M. Vandichel, K. Houthoofd, A. Vimont, M. Daturi, M. Waroquier, V. Van Speybroeck, D.E. de Vos, Synthesis Modulation as a Tool To Increase the Catalytic Activity of Metal-Organic Frameworks: The Unique Case of UiO-66(Zr), J. Am. Chem. Soc. 135 (2013) 11465–11468, https://doi.org/10.1021/ja405078u.
[26] H.H. Mautschke, F. Drache, I. Senkovska, S. Kaskel, F.X. Llabrés i Xamena, Catalytic properties of pristine and defect-engineered Zr-MOF-808 metal organic frameworks, Catal. Sci. Technol. 8 (2018) 3610–3616, https://doi.org/10.1039/C8CY00742J.
[27] E. Plessers, G. Fu, C.Y.X. Tan, D.E. de Vos, M.B.J. Roeffaers, Zr-Based MOF-808 as Meerwein–Ponndorf–Verley Reduction Catalyst for Challenging Carbonyl Compounds, Catalysts 6 (2016) 104, https://doi.org/10.3390/catal6070104.
[28] A.H. Valekar, M. Lee, J.W. Yoon, J. Kwak, D.Y. Hong, K.R. Oh, G.Y. Cha, Y. U. Kwon, J. Jung, J.S. Chang, Y.K. Hwang, Catalytic Transfer Hydrogenation of Furfural to Furfuryl Alcohol under Mild Conditions over Zr-MOFs: Exploring the Role of Metal Node Coordination and Modification, ACS Catal. 10 (2020) 3720–3732, https://doi.org/10.1021/acscatal.9b05085.
[29] S. Rojas-Buzo, P. Garcia-Garcia, A. Corma, Catalytic Transfer Hydrogenation of Biomass-Derived Carbonyls over Hafnium-Based Metal–Organic Frameworks, ChemSusChem. 11 (2018) 432–438, https://doi.org/10.1002/cssc.201701708.
[30] A.H. Valekar, K.H. Cho, S.K. Chitale, D.Y. Hong, G.Y. Cha, U.H. Lee, D.W. Hwang, C. Serre, J.S. Chang, Y.K. Hwang, Catalytic transfer hydrogenation of ethyl levulinate to γ-valerolactone over zirconium-based metal–organic frameworks, Green Chem. 18 (2016) 4542–4552, https://doi.org/10.1039/C6GC00524A.
[31] A.H. Valekar, K.R. Oh, Y.K. Hwang, Chemoselective Transfer Hydrogenation of Flavoring Unsaturated Carbonyl Compounds over Zr and Hf-based Metal-Organic Frameworks, Bull. Korean Chem. Soc. 42 (2021) 467–470, https://doi.org/10.1002/bkcs.12226, 2021.

[32] Y. Lin, Q. Bu, J. Xu, X. Liu, X. Zhang, G.P. Lu, B. Zhou, Hf-MOF catalyzed Meerwein-Ponndorf-Verley reduction reaction: Insight into reaction mechanism, Mol. Catal. (2021), 111405, https://doi.org/10.1016/j.mcat.2021.111405.
[33] F.G. Cirujano, F.X. Llabrés i Xamena, Tuning the Catalytic Properties of UiO-66 Metal-Organic Frameworks: From Lewis to Defect-induced Brønsted Acidity, J. Phys. Chem. Lett. 11 (2020) 4879–4890, https://doi.org/10.1021/acs.jpclett.0c00984.
[34] C. Caratelli, J. Hajek, F.G. Cirujano, M. Waroquier, F.X. Llabrés i Xamena, V. Van Speybroeck, Nature of active sites on UiO-66 and beneficial influence of water in the catalysis of Fischer esterification, J. Catal. 352 (2017) 401–414, https://doi.org/10.1016/j.jcat.2017.06.014.
[35] C.A. Trickett, T.M.O. Popp, J. Su, C. Yan, J. Weisberg, A. Huq, P. Urban, J. Jiang, M.J. Kalmutzki, Q. Liu, J. Baek, M.P. Head-Gordon, G.A. Somorjai, J.A. Reimer, O. M. Yaghi, Identification of the strong Brønsted acid site in a metal–organic framework solid acid catalyst, Nat. Chem. 11 (2019) 170–176, https://doi.org/10.1038/s41557-018-0171-z.
[36] J. Jiang, O.M. Yaghi, Brønsted Acidity in Metal−Organic Frameworks, Chem. Rev. 115 (2015) 6966–6997, https://doi.org/10.1021/acs.chemrev.5b00221.
[37] R.C. Klet, Y. Liu, T.C. Wang, J.T. Hupp, O.K. Farha, Evaluation of Brønsted acidity and proton topology in Zr- and Hf-based metal–organic frameworks using potentiometric acid–base titration, J. Mater. Chem. A 4 (2016) 1479–1485, https://doi.org/10.1039/c5ta07687k.
[38] A. Herbst, A. Khutia, C. Janiak, Brønsted Instead of Lewis Acidity in Functionalized MIL-101Cr MOFs for Efficient Heterogeneous (nano-MOF) Catalysis in the Condensation Reaction of Aldehydes with Alcohols, Inorg. Chem. 53 (2014) 7319–7333, https://doi.org/10.1021/ic5006456.
[39] J. Jiang, F. Gándara, Y.B. Zhang, K. Na, O.M. Yaghi, W.G. Klemperer, Superacidity in Sulfated Metal−Organic Framework-808, J. Am. Chem. Soc. 136 (2014) 12844–12847, https://doi.org/10.1021/ja507119n.
[40] X. Li, L. Huang, A. Kochubei, J. Huang, W. Shen, H. Xu, Q. Li, Evolution of a Metal-Organic Framework into a Brønsted Acid Catalyst for Glycerol Dehydration to Acrolein, ChemSusChem. 13 (2020) 5073–5079, https://doi.org/10.1002/cssc.202001377.
[41] Q. Zhao, W.H. Chen, S.J. Huang, Y.C. Wu, H.K. Lee, S.B. Liu, Discernment and Quantification of Internal and External Acid Sites on Zeolites, J. Phys. Chem. B 106 (2002) 4462–4469, https://doi.org/10.1021/jp015574k.
[42] W.H. Chen, H.H. Ko, A. Sakthivel, S.J. Huang, S.H. Liu, A.Y. Lo, T.C. Tsai, S. Bin Liu, A solid-state NMR, FT-IR and TPD study on acid properties of sulfated and metal-promoted zirconia: Influence of promoter and sulfation treatment, Catal. Today 116 (2006) 111–120, https://doi.org/10.1016/j.cattod.2006.01.025.
[43] L. Baltusis, J.S. Frye, G.E. Maciel, Phosphine oxides as NMR probes for adsorption sites on surfaces, J. Am. Chem. Soc. 108 (2002) 7119–7120, https://doi.org/10.1021/ja00282a055.
[44] Y. Jiang, J. Huang, W. Dai, M. Hunger, Solid-state nuclear magnetic resonance investigations of the nature, property, and activity of acid sites on solid catalysts, Solid State Nucl. Magn. Reson. 39 (2011) 116–141, https://doi.org/10.1016/j.ssnmr.2011.03.007.
[45] A. Zheng, S. Bin Liu, F. Deng, ^{31}P NMR Chemical Shifts of Phosphorus Probes as Reliable and Practical Acidity Scales for Solid and Liquid Catalysts, Chem. Rev. 117 (2017) 12475–12531, https://doi.org/10.1021/acs.chemrev.7b00289.
[46] F.G. Cirujano, A. Corma, F.X. Llabrés i Xamena, Conversion of levulinic acid into chemicals: Synthesis of biomass derived levulinate esters over Zr-containing MOFs, Chem. Eng. Sci. 124 (2015) 52–60, https://doi.org/10.1016/j.ces.2014.09.047.
[47] M. Kandiah, M.H. Nilsen, S. Usseglio, S. Jakobsen, U. Olsbye, M. Tilset, C. Larabi, E.A. Quadrelli, F. Bonino, K.P. Lillerud, Synthesis and Stability of Tagged UiO-66 Zr-MOFs, Chem. Mater. 22 (2010) 6632–6640, https://doi.org/10.1021/cm102601v.
[48] H. Furukawa, F. Gandara, Y.B. Zhang, J. Jiang, W.L. Queen, M.R. Hudson, O. M. Yaghi, Water Adsorption in Porous Metal−Organic Frameworks and Related Materials, J. Am. Chem. Soc. 136 (2014) 4369–4381, https://doi.org/10.1021/ja500330a.